Dynamics of resonant charge transfer in low-energy alkali-metal-ion scattering

G. A. Kimmel and B. H. Cooper
Laboratory of Atomic and Solid State Physics, Cornell University, Ithaca, New York 14853-2501
(Received 11 February 1993)

We show in this paper that measurements of charge-state distributions for 5–1600 eV Li, Na, and K scattered from a clean Cu(001) surface provide an excellent probe of the dynamics of atom-surface charge transfer. The neutralization probabilities, measured as a function of the perpendicular velocities of the scattered atoms, are qualitatively different for the three species. These differences reflect the high sensitivity of the charge transfer in this energy range to the energies and lifetimes of the atomic resonances near the surface. The measured neutralization probabilities are found to depend on the parallel velocity component of the scattered atom, even though the velocities at which these experiments are conducted are relatively low. The data are compared to several models of the charge-transfer process. Agreement with the data is achieved using a model based on the one-electron Newns-Anderson Hamiltonian and using calculated values for the alkali-metal resonance parameters.

I. INTRODUCTION

Charge transfer, or the exchange of electrons, is a crucial step in many processes involving dynamical interactions of atoms and molecules with surfaces. Among them are chemisorption, electron-stimulated desorption, laser-induced desorption, and dissociative scattering. Charge exchange is also important in a number of technological applications such as thin-film growth by chemical vapor deposition, reactive ion etching, surface catalysis, and secondary-ion mass spectroscopy (SIMS). Because of its importance in such a wide range of problems, the mechanisms of charge transfer have been studied extensively.[1–21]

Many dynamical processes at surfaces and charge transfer in particular depend on, among other things, the energies and lifetimes of the atomic and molecular states (resonances) in the vicinity of the surface. For example, a molecule might dissociatively chemisorb on a surface if the lowest unoccupied molecular orbital (an antibonding orbital) lies below the Fermi level and is filled when the molecule approaches the surface.[22] In another example, the desorption of neutral NO from Pt(111) when the surface is irradiated with laser light has been attributed to the formation of a negative-ion (NO^{-1}) intermediary at the surface.[23] The lifetime of the negative-ion intermediary is important in determining the desorption probability and the vibrational state distribution of the desorbed molecules.

In general, the lifetimes and energies of the atomic and molecular resonances in the vicinity of the surface play an important role in determining the outcome of charge-transfer processes. These lifetimes and energies, which are parameters in the theories of charge transfer, are hard to calculate theoretically and difficult to probe experimentally.[16] However, we will show in this paper that atomic beam scattering experiments provide an excellent method for studying the dynamics of charge exchange.

We have measured neutralization probabilities for Li, Na, and K scattered from clean Cu(001) along the ⟨100⟩ azimuth for a range of scattered atom velocities. From energetic considerations, the adiabatic charge states for Li and Na in the Li+Cu and Na+Cu systems are neutral when the atoms are far from the surface, while for the K+Cu system the K is positively ionized. We find that the Li and K monotonically approach the adiabatic charge states as the scattered atom velocity decreases. However, for Na the neutralization probability is *non-monotonic;* it initially decreases with decreasing velocity and then increases, approaching the adiabatic ground state at the lowest velocities.

The Li and K data and the somewhat surprising behavior for Na reflect the high sensitivity of the charge-transfer dynamics in this velocity range to the lifetimes and energies of the atomic resonances in the vicinity of the surface. We have calculated the neutralization using various models of resonant charge exchange which will be described below. In principle, constraints on the possible values for the lifetimes and energies of atomic resonances can be found by comparing the calculated and measured neutralization probabilities. We will show that good agreement between theory and data can be obtained using alkali-metal resonance lifetimes and energies calculated by Nordlander and Tully.[20,24]

The models discussed below consider only the resonant charge exchange process. However, other processes such as Auger and radiative neutralization are also possible. In addition, recent studies have shown that core-level excitations produced in collisions between the scattered atom and a substrate atom can leave the scattered atom in a long-lived autoionizing state,[25,26] which subsequently deexcites far from the surface where it can no longer be neutralized, thus enhancing the scattered ion fraction.

Radiative neutralization is expected to be small compared to resonant processes due to the long lifetimes for radiative transitions. The relative importance of Auger neutralization is not so easily assessed. In some cases, Auger and resonant neutralization rates may be comparable.[4,27–29] However, since the alkali-metal valence levels (the outer *s* orbitals) are similar in energy to the metal

0163-1829/93/48(16)/12164(14)/$06.00

Fermi level, the electrons created in the metal due to an Auger transition may not have enough energy to escape the bulk, making direct observation of Auger neutralization difficult. A further complication is that some models of resonant and Auger charge transfer predict the same velocity dependence for the neutralization of the scattered atoms.

For alkali-metal ion scattering, most treatments assume that the resonant neutralization dominates. We will see that we can adequately account for the neutralization of Li, Na, and K scattered from Cu(001) in the energy range from 5 to 1600 eV with a theory of resonant charge exchange based on the Newns-Anderson Hamiltonian, which does not include Auger or radiative neutralization, or neutralization into excited states of the scattered atom.

In Sec. II, we will describe the equipment and method used for obtaining the neutralization data. In Sec. III, we will review a simple picture of the resonant charge exchange which is useful for interpreting the qualitative features of the data. We will also review the theory of resonant charge exchange which is based on the Newns-Anderson Hamiltonian. In Sec. IV, we will compare the experimental results to the model with the goal of extracting information about the lifetimes and energies of the atomic resonances. The effect of the scattered atom's parallel velocity on the neutralization is considered in Sec. V. Finally, conclusions are drawn in Sec. VI.

II. EXPERIMENTAL EQUIPMENT AND METHOD

The experiments were performed in an ultrahigh vacuum (UHV) system which has been described elsewhere.[30–32] Only the relevant details are presented here. The UHV chamber is equipped with a beamline capable of producing well-collimated monoenergetic ion beams in the energy range from 5 eV to 10 keV. In the experiments described in this paper, we used Li, Na, and K ions with incident energies from 5 to 1600 eV. The base pressure for the scattering chamber is 1×10^{-10} Torr. Typical operating pressures are $(2-3)\times10^{-10}$ Torr. All measurements were performed on a clean Cu(001) surface, prepared by standard sputter and anneal cycles. The surface order and cleanliness were checked with low-energy electron diffraction (LEED) and Auger-electron spectroscopy (AES), respectively. The scattered atoms are detected with a time-of-flight (TOF) spectrometer, mounted on a rotatable platform, which can be used to make velocity- and angle-resolved measurements of neutral and ionized alkali-metal atoms.[32] This spectrometer is described below.

In order to detect low-energy neutral alkali-metal atoms, we adapted a technique used by van Amersfoort *et al.*[15] The main elements of the TOF spectrometer include a set of collimation apertures, a platinum foil, a pair of biasing elements, and a channel electron multiplier. To measure the total flux of scattered atoms, the detector is positioned at the desired total scattering angle. The scattered atoms (neutrals and ions) pass through the collimation apertures, and then scatter off a clean platinum foil. The platinum foil efficiently ionizes the atoms, regardless of their incident charge states. These ions are then accelerated to a high energy where they strike the conversion dynode of the channel electron multiplier.

The flux of neutral atoms scattered from the Cu sample can be detected by biasing an aperture located in front of the collimation apertures, which rejects the scattered ion flux but transmits the neutrals. The angle-resolved neutral fraction of the alkali-metal atoms scattered from the Cu sample is then given by the ratio of the neutral flux to the total flux. Because the atoms lose memory of their initial charge states during their interactions with the Pt foil (see the discussion in Sec. IV), ions and neutrals are detected with the same efficiency. The incident ion beam is pulsed using a set of electrostatic deflection plates, and the times of arrival of the scattered atoms are measured so that their velocities can be determined.

Figure 1 shows measured TOF spectra for 400-eV Na^+ scattered along the $\langle 100\rangle$ azimuth of Cu(001), with the beam incident at an angle $\theta_i=45°$ from the sample normal and the detector located at a final angle $\theta_f=45°$, also measured from the sample normal. The intensity versus time of arrival is shown both for the total flux, i.e., ions plus neutrals (solid line), and for the neutrals only (dashed line). Three peaks are clearly discernible in each of the spectra. They correspond to trajectories involving collisions with atoms in the top layer of the surface; the peak at the smallest time of arrival corresponds to quasidouble (QD) and zigzag (ZZ) trajectories, the middle peak to zigzag trajectories, and the peak at the largest time of arrival to quasisingle trajectories (QS).[33,34]

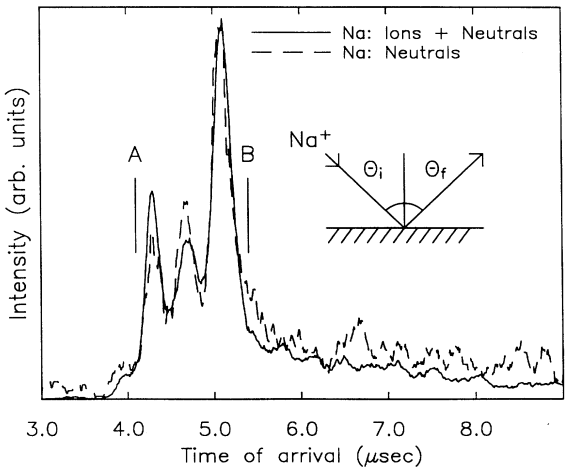

FIG. 1. Time-of-flight (TOF) spectra of scattered Na atoms for 400-eV Na^+ incident on Cu(001) along the $\langle 100\rangle$ azimuth with $\theta_i=\theta_f=45°$. The intensity versus time of arrival for the scattered neutral flux (dashed line) and total scattered flux (solid line) are shown. The two spectra, which are similar, each have three prominent peaks; in order of increasing time of arrival they are due to quasidouble (QD) and zigzag (ZZ), zigzag, and quasisingle (QS) scattering events. The spectra have been scaled so that the QS peaks are the same height. The neutrals account for ~5% of the total scattered flux. The intensity at lower energies (longer times) is due to more complicated scattering events. The neutralization probability is calculated by taking the ratio of the integrated intensities in the two spectra.

In Fig. 2, the TOF spectra for the total flux (solid line) and neutral flux (dashed line) from Fig. 1 are replotted as a function of the perpendicular velocities, $v_\perp$, of the scattered atoms.[35] Also plotted is the apparent neutralization probability (i.e., the ratio of the neutral to the total flux) as a function of $v_\perp$ for these spectra (solid circles). At the lower velocities, the apparent neutralization probability increases dramatically. This portion of the spectrum includes complicated scattering trajectories, and may include some contribution from sputtered atoms. When neutralization probabilities are presented elsewhere in this paper they are calculated from the three well-defined peaks in the TOF spectra (e.g., involving the QS, ZZ, and QD scattering trajectories, as discussed above).

In principle, the trajectories in the three peaks should have different neutralization probabilities since they have different final velocities. In practice, the neutralization probabilities for the different trajectories with a given incident energy are small compared to the changes in the neutralization that occur as the incident energy is changed. (For example in Fig. 2, the neutralization for the three peaks is quite similar.) As a result, for a given scattering geometry and incident energy, the neutralization probability is found by taking the ratios of the integrated intensities associated with the three main peaks in the neutral and total spectra; e.g., in Fig. 1, the neutral fraction is found by integrating from points A to B in the neutral and total spectra and taking the ratio of these two quantities. The velocity associated with that neutralization probability is taken as the weighted average velocity of the spectrum in the range from A to B. Then by changing the incident energy and the scattering geometry, we can measure the neutralization as a function of the velocity of the scattered atoms.

Figure 3 shows the measured neutralization probabilities as a function of the perpendicular velocities of the scattered atoms for Li, Na, and K scattered along the $\langle 100 \rangle$ azimuth of Cu(001) with $\theta_i = \theta_f = 55°$. The observed behavior is qualitatively different in each case. For K, essentially no neutralization is seen. For Li the neutralization monotonically decreases as the final perpendicular velocity increases. For Na, on the other hand, the neutralization goes through a minimum in the velocity range investigated.

The estimated uncertainty in the data is also indicated in Fig. 3. Each data point is typically the average of several measurements and the error is taken to be the standard deviation of the individual measurements. For any individual measurement, the error due to counting statistics is small compared to the other sources of experimental error.

One of the primary sources of error is due to changes in the intensity of the incident ion beam with time. Since measurements of the total and neutral fluxes are made in a repeated, alternating sequence over a period of time (usually about 10 min), changes in the incident beam intensity introduce errors into the determination of the neutralization probability. The beams tend to become less stable as the incident energy decreases, therefore the uncertainty increases somewhat at the lower energies. In general, however, the reproducibility of the data is quite good.

Finally, at the very lowest energies in our experiments, differences in the ion and neutral trajectories in the TOF spectrometer, which are due primarily to the interaction between the ions and their image charges in the Pt foil,[32]

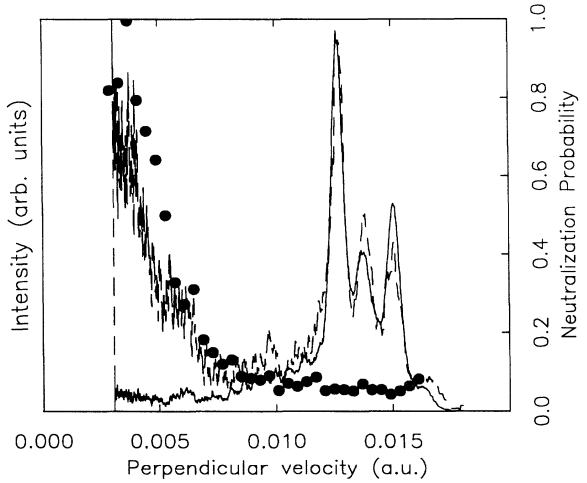

FIG. 2. Neutralization probability versus perpendicular velocity (solid circles) of the scattered atoms for 400-eV Na^+ incident on Cu(001) along the $\langle 100 \rangle$ azimuth, with $\theta_i = \theta_f = 45°$. The velocities are expressed in atomic units (a.u.). The TOF spectra from Fig. 1 are also shown for reference. The neutralization probabilities for the three main peaks are all similar. An increase in the measured neutral fraction at low velocities is observed; this portion of the spectrum includes complicated scattering trajectories. (This figure shows lower velocities than Fig. 1.)

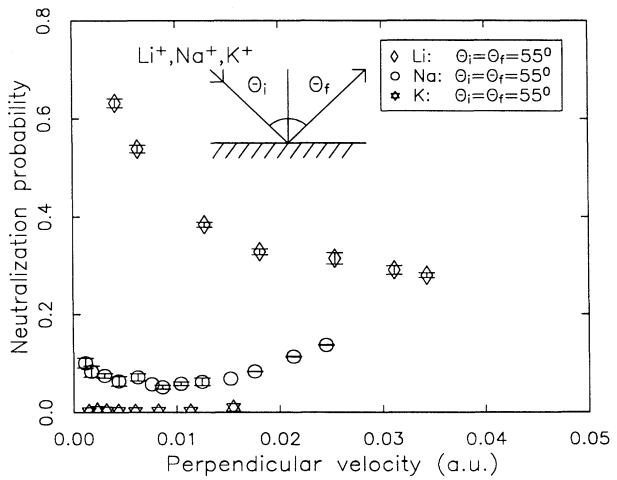

FIG. 3. Neutralization probability versus perpendicular velocity of the scattered atoms for Li^+, Na^+, and K^+ incident on Cu(001) along the $\langle 100 \rangle$ azimuth, with $\theta_i = \theta_f = 55°$. These curves represent data taken for a number of incident beam energies; they are 10–1200 eV for Li, 5–1200 eV for Na, and 10–1600 eV for K. In general the neutralization probability decreases as the energy of the ionization level of the atom [e.g., Li(2s), Na(3s), K(4s)] increases. Note also that the neutralization versus perpendicular velocity is qualitatively different for the three species (see the text).

might be expected to affect the accuracy of the spectrometer. At present, we do not know at what energy the ions and neutrals begin to have different detection efficiencies due to this effect, but it appears to be lower than 10 eV. Thus, this possibility does not influence any of the conclusions in this paper.

III. THEORY OF RESONANT CHARGE TRANSFER

In this section we will discuss a simple qualitative picture of the resonant charge-transfer process which is useful for understanding the trends seen in the Li, Na, and K data in Fig. 3. This is followed by a brief review of a theory of resonant charge transfer based on the Newns-Anderson Hamiltonian. Both the simple picture and the theory have been discussed previously in the literature.[1,2,7,36] In Sec. IV, we will compare the results of these theories to the data with the goal of investigating the sensitivity of the neutralization to the lifetimes and energies of the atomic states in the vicinity of the metal surface.

A. Qualitative model

We are concerned with the nonadiabatic transfer of electrons between an atomic orbital and a metal surface. For the case of alkali-metal atoms interacting with a clean copper surface, we shall assume initially that only the outer s orbital of the alkali-metal atom is important in the charge transfer.

The interaction with the surface broadens the atomic state, turning it into a resonance. This broadening, which is due to the overlap of the atomic wave function with the metallic wave functions, increases as the atom approaches the surface. The width of the resonance increases roughly exponentially with decreasing atom-surface separation since the metallic wave functions decay exponentially into the vacuum.[20,37] The interaction of the atom with the surface also shifts the energy of the atomic resonance. At the distances where the charge transfer is most likely to occur (see the discussion of the freezing distance below), this shift is usually adequately represented by the classical image shift.[37] In this approximation, the energy of the atomic resonance $\epsilon_a(z)$ is given by (all equations are in atomic units)

$$\epsilon_a(z) = -I + \frac{1}{4(z - z_{\rm im})} , \tag{1}$$

where I is the ionization potential of the atom (measured from the vacuum), z is the atom-surface separation ($z=0$ corresponds to the jellium edge), and $z_{\rm im}$ is the location of the image plane. It is often assumed that the half-width of the atomic resonance, $\Delta(z)$, is given by

$$\Delta(z) = \Delta_0 e^{-\alpha z} . \tag{2}$$

As we will see, the charge-transfer probability is very sensitive to $\Delta(z)$ and $\epsilon_a(z)$.

Since this is a nonadiabatic problem, we must concern ourselves with various time scales. There are two of particular interest; the first is the lifetime of the resonance which is inversely proportional to the coupling, $\tau_r = 1/2\Delta(z)$. The second is the time scale for the atom to scatter from the surface, which is inversely proportional to the component of the atom's velocity that is perpendicular to the surface, $\tau_v = 1/(\alpha v_\perp)$. Since the atom's velocity is approximately constant in the region where charge transfer is most likely to occur, the timescale for the motion is constant.[38] The lifetime of the atomic resonance, however, varies with distance outside the surface.

Far from the surface, the coupling between the atom and the metal is weak (decaying exponentially with increasing atom-surface separation), and $\tau_r \gg \tau_v$. In this case, no charge transfer occurs. Close to the surface, on the other hand, the coupling is very strong, and $\tau_r \ll \tau_v$.[2] In the latter case, the atom quickly loses memory of its incident charge state.[39] The final charge state of the atom is then determined on the outgoing trajectory approximately at the "freezing distance" where these two time scales are equal, i.e., $\tau_r = \tau_v$, and it reflects the occupancy of the atomic resonance at the freezing distance.[7,36] The freezing distance is given by

$$z_{\rm fr} = \frac{1}{\alpha} \ln \left[\frac{2\Delta_0}{\alpha v_\perp} \right] . \tag{3}$$

The concept of a freezing distance is relevant because the width of the atomic resonance decreases exponentially with distance from the surface so that only a relatively small range of distances is important in determining the final charge state of the atom. This leads to a simple picture which contains some of the important physics for understanding the charge-transfer process.

As the velocity of the scattered atom increases, τ_v decreases and the freezing distance decreases. Therefore, changing the velocity of the atom probes the occupancy of the atomic level as a function of distance outside the surface. The occupancy of the level depends on both the energy of the level relative to the Fermi level and on the width of the level. Thus, by measuring the neutralization probability as a function of the velocity of the scattered atoms, we can investigate the widths of the atomic resonances near the surface. (Several effects which complicate the determination of the widths will be discussed below.)

In Fig. 3 we saw that the measured neutralization probabilities versus perpendicular velocity were quite different for Li, Na, and K, both qualitatively and quantitatively. These different behaviors are related to the different level widths and the energies of the Li($2s$), Na($3s$), and K($4s$) orbitals relative to the work function for clean Cu(001), which is 4.59 eV.[40] For K, the first ionization potential is 4.34 eV. Since the interaction with the surface increases the energy of the K($4s$) level [Eq. (1)], it is energetically favorable for the K($4s$) level to be empty over a wide range of atom-surface separations (i.e., the broadened $4s$ resonance lies predominantly above the copper Fermi level). As a result, almost no neutralization is seen for K. For Li, the first ionization potential is 5.39 eV. The Li($2s$) level is below the Fermi level far from the surface and above it close to the surface. In the velocity range of the experiment, the freezing distance changes from where the resonance is predominantly below the

Fermi level (lower velocities) to predominantly above the Fermi level (higher velocities). Thus the neutralization probability decreases significantly as the velocity of the scattered Li increases.

The charge-transfer behavior for Na is intermediate between these two cases. The first ionization potential is 5.14 eV, so the Na(3s) resonance is, as in the case of Li, predominantly below the Fermi level far from the surface and predominantly above it close to the surface. For Na, however, there is considerably less neutralization than in the case of Li and the neutralization does not monotonically decrease as the scattered velocity increases. Instead, it goes through a *minimum,* increasing again at higher velocities. The minimum is due to the exponential increase in the level width with decreasing atom-surface separation. (The influence of other factors on the minimum will be discussed later in the paper.) For Na, the increase in the width is relatively more important at higher velocities than the shift in the energy of the level due to the image interaction. As a result, as the velocity increases and the freezing distance decreases, more of the resonance lies below the Fermi level and the neutralization increases, even though the centroid of the resonance is at a higher energy.

In gas phase scattering, the probability to make a charge transfer can also exhibit a maximum (or minimum) as a function of the relative velocity of atoms.[41] This type of process is not related to the minimum which we find in the neutralization of Na as a function of velocity. In atom-atom scattering, only a limited number of states (i.e., two for the cases of interest) participate in the charge exchange. As a result, the atoms do not lose memory of the charge state before the collision. In fact, the nonmonotonic behavior is closely related to the charge-transfer probabilities on both the incident and exit trajectories. In atom-surface scattering, on the other hand, the atomic state interacts with a continuum of metallic states which effectively erase the memory of any charge exchange on the incident trajectory. As a result, the nonmonotonic behavior is related to the dynamics of the charge-transfer process on the outgoing trajectory only. We will consider other possible explanations for the nonmonotonic behavior in Sec. V.

B. Quantitative model

While the concept of a freezing distance provides a useful qualitative picture, it cannot be used to quantitatively model the dynamics of the charge-transfer process. For a more quantitative picture (which does *not* assume a freezing distance), we will use the Newns-Anderson Hamiltonian which has been used to model resonant charge exchange.[1,2]

The model assumes that only a single spinless atomic orbital participates in the charge-transfer process, and therefore it rules out two electron processes such as Auger neutralization. It also ignores neutralization into excited states and the formation of negative ions.

The Newns-Anderson Hamiltonian is

$$H(t)=\sum_k \epsilon_k n_k+\epsilon_a(t)n_a+\sum_k [V_{ak}(t)c_a^\dagger c_k+\text{H.c.}] , \quad (4)$$

where ϵ_k and ϵ_a are the energies of the metal electronic levels and the atomic level, respectively. n_k and n_a are the corresponding number operators, $n_i=c_i^\dagger c_i$. V_{ak} is $\langle a|V|k\rangle$ with V representing the coupling of the atomic state to those in the metal.

The k and time dependence of $V_{ak}(t)$ are assumed to be separable,[2] i.e., $V_{ak}(t)=u(t)V_{ak}$. The half-width of the atomic resonance [recall Eq. (2)] is defined as

$$\Delta(\epsilon,z)\equiv\pi\sum_k |V_{ak}|^2\delta(\epsilon-\epsilon_k) . \quad (5)$$

Using the broadband approximation, where $\Delta(\epsilon,z)=\Delta(z)$, the occupancy of the atomic state as a function of time, $n_a(t)$, is found by Brako and Newns (BN) to be[2]

$$n_a(t)=n_a(t_0)\exp\left[-2\int_{t_0}^{t}\Delta(t')dt'\right]+\frac{1}{\pi}\int d\epsilon\, f(\epsilon,T)\left|\int_{t_0}^{t}\sqrt{\Delta(t')}\exp\left[-i\epsilon t'-\int_{t'}^{t}[i\epsilon_a(t'')+\Delta(t'')]dt''\right]dt'\right|^2 , \quad (6)$$

where f is the Fermi function, and $\epsilon_a(t)$ and $\Delta(t)$ give the time dependence of the energy and width of the atomic resonance due to the motion of the scattered atom. For the rest of the paper, Eq. (6) will be referred to as the "BN" model.

The first term in Eq. (6) arises from the decay of the initially filled level [if $n_a(t_0)=1$] into the continuum of metal states at a rate $\Delta(t)$. The role of this "memory" term has been discussed elsewhere.[2] For our ion scattering experiments, $n_a(t_0)=0$ and the memory term is zero (i.e., the incident particle is an ion).

As mentioned above, several important approximations are made in the solution of the Newns-Anderson Hamiltonian [Eq. (6)]; the spin degeneracy of the atomic state is neglected, and only one atomic state is considered. Recently, a considerable amount of theoretical work has been done to extend the solutions of the generalized Newns-Anderson Hamiltonian to eliminate these approximations.[10,42–45] There are charge exchange experiments which provide a good test of these more sophisticated models, such as those measuring the formation of negative and excited neutral Li at low work-function surfaces.[45–49] However, for the experiments described in this paper the results of the more sophisticated model are qualitatively similar to those of the BN model.[45]

IV. RESULTS AND DISCUSSION

We saw above that a very simple picture of the neutralization process could be used to understand the qualitative behavior for Li, Na, and K. Recall that the velocity dependence of the neutralization probability was sensitive to the lifetimes and energies of the atomic resonances. In this section, we will compare the experimental data for

the neutralization of alkali-metal atoms scattered from Cu(001) to the results of the BN model [Eq. (6)] in order to investigate this sensitivity in more detail. Since the scattering experiments are performed with a range of incident energies, the experimental results are sensitive to the lifetime over a range of distances outside the surface. Therefore, to achieve agreement between the theory and the data, the calculated lifetimes and energies need to be correct for a range of distances.

Figure 4 shows the measured neutralization probability versus perpendicular velocity for Li along with that calculated using the BN model [Eq. (6)]. In Fig. 4, tabulated values for the lifetime and energy of the Li($2s$) resonance, calculated by Nordlander and Tully, were used in the model (solid line).[20,50] The BN model, which in this case has no free parameters, does an excellent job of reproducing the data.

The BN model is quite sensitive to the lifetime of the atomic resonance. Figure 4 shows that increasing or decreasing $\Delta(z)$ by a factor of 2 results in significant changes in the final neutralization probability.

However, as we will show, the results of the charge-transfer model are relatively insensitive to the lifetimes and energies of the atomic resonance very close to the surface. The lifetimes and energies calculated by Nordlander and Tully are reported for $z \geq 5$ a.u.[20,50] For our modeling, we have extrapolated their calculations to smaller atom-surface separations. Most calculations of the resonance lifetimes show that they saturate close to the surface. We have calculated neutralization probabilities for Li using two different parameterizations of the Li($2s$) lifetime. The first assumes an exponential form for the level width, as in Eq. (2), where the parameters Δ_0 and α are chosen to give the best fit of the exponential to the calculations of Nordlander and Tully[20,50] over the range $6a_0 \leq z \leq 12a_0$ (i.e., the approximate range of freezing distances in the experiments). (In that case, the value of Δ_0 *does not* represent the width of the resonance at the surface. A typical value at the surface would be ~ 1 eV,[37] which is much smaller than Δ_0.) The second parametrization uses a form of $\Delta(z)$ which saturates close to the surface and decays exponentially farther away,

$$\Delta(z)=\frac{\Delta_0}{\left[e^{4\alpha z}+\left[\frac{\Delta_0}{\Delta_{\rm sat}}\right]^4\right]^{1/4}} . \tag{7}$$

For $z \rightarrow 0$, $\Delta(z) \rightarrow \Delta_{\rm sat}$ provided that $\Delta_0 \gg \Delta_{\rm sat}$ which is typically true. For $\Delta_{\rm sat} \rightarrow \infty$, the simple exponential form [Eq. (2)] is obtained.

Figure 5 shows calculations of the Li neutralization probability using these two different parametrizations of the resonance width. The exponential parametrization gives results which are very similar to the results in Fig. 4, where tabulated values for the level width were used. Saturating the width affects the neutralization at higher velocities where the charge state is determined closer to the surface. At lower velocities, the atom loses memory of the charge state (and therefore the width) near the surface.

Figure 6 shows the measured as well as calculated neutralization probability for Na as a function of the perpen-

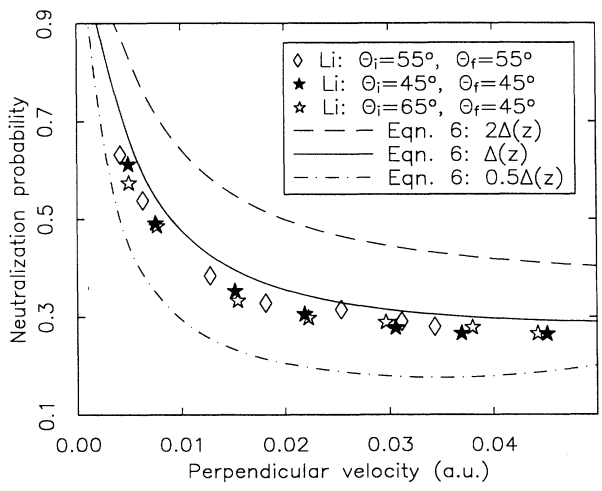

FIG. 4. Comparison of measured Li neutralization probabilities with calculations using the BN model [Eq. (6)]. The measured Li neutralization probability versus perpendicular velocity is shown for three different scattering geometries. The resonance width $\Delta(z)$ and energy $\varepsilon_a(z)$ are from calculations by Nordlander and Tully (Refs. 20 and 50). Tabulated values of $\Delta(z)$ and $\varepsilon_a(z)$ were used in Eq. (6) without substituting a fit to the analytical forms [Eqs. (1) and (2)] often used for these quantities. Agreement with the data is good over the entire velocity range of the experiment. The BN model is very sensitive to the resonance widths; increasing (dashed line) or decreasing (dash-dotted line) $\Delta(z)$ by a factor of 2 changes the results of the model significantly.

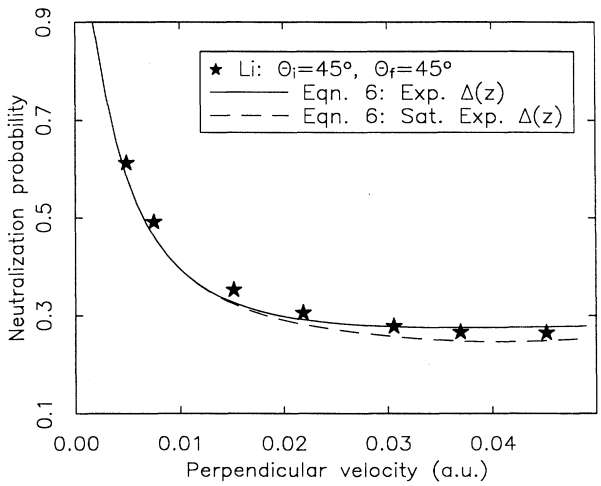

FIG. 5. Comparison of the measured lithium neutralization probability versus perpendicular velocity with calculations using the BN model [Eq. (6)] with two different forms for the resonance width $\Delta(z)$. The solid line shows the results of the calculation assuming $\Delta(z)$ is given by an exponential [Eq. (2)], while the dashed line shows the results using a resonance width which saturates close to the surface [Eq. (7)]. The two calculated curves differ only at higher velocities where the freezing distance is small and the final charge state is determined closer to the surface, and where the two forms of $\Delta(z)$ differ from one another.

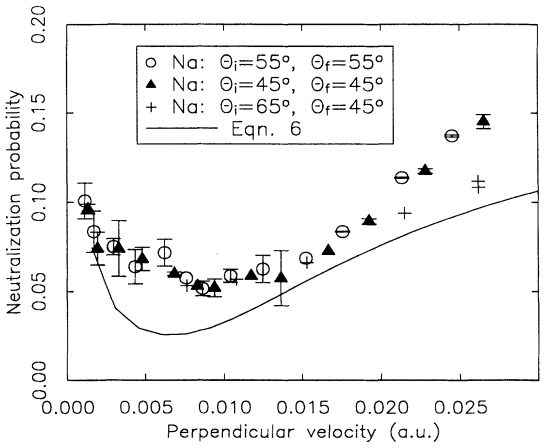

FIG. 6. Measured neutralization probability versus perpendicular velocity of Na, for three different scattering geometries, compared to calculations using the BN model [Eq. (6)]. The resonance width $\Delta(z)$ and energy $\varepsilon_a(z)$ used in the model were from calculations by Nordlander and Tully (Refs. 20 and 50). The model, which has no free parameters, agrees with the data.

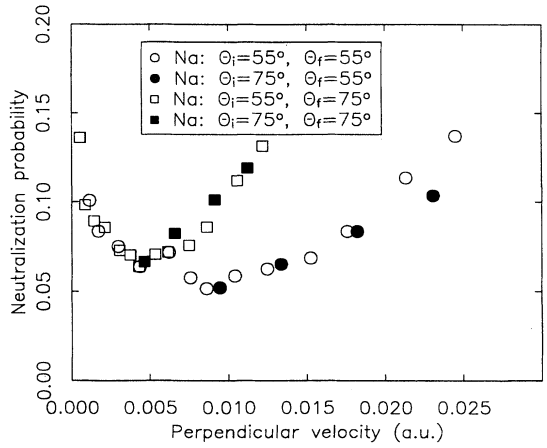

FIG. 7. Measured neutralization probability versus perpendicular velocity for Na for four different scattering geometries. For a given final scattering angle, the neutralization is the same regardless of the incident scattering angle. However, the neutralization changes when the final scattering angle is changed.

dicular velocity of the scattered atom. The measurements are made for three different scattering geometries. As mentioned previously, the neutralization goes through a minimum in the velocity range investigated. The calculations were again performed using the BN model [Eq. (6)] with tabulated energies and lifetimes of the Na($3s$) level taken from the calculations of Nordlander and Tully.[20,50] The agreement between the model and the data is reasonably good. Note that the model also gives a minimum in the neutralization. The increasing neutralization at higher velocities reflects, among other things, the increasing width of the resonance with decreasing distance from the surface. As will be seen later, the shape of the neutralization curve in the vicinity of the minimum also depends on the atom's parallel velocity.

In Sec. III, we discussed the "memory" of the incident charge state during resonant charge exchange. Calculations with the BN model indicate that the atom loses memory of its initial charge state and its charge state on the incoming trajectory. Also, since the width and energy of the resonance are assumed to depend only on z, and not on the lateral position of the atom, the BN model depends only on the perpendicular component of the velocity of the scattered atom.

The assumptions regarding the loss of memory and the velocity dependence can be tested experimentally by changing the scattering geometry. In Figs. 4 and 6, we saw that the neutralization probability for Li and Na for $\theta_f=45°$ was the same when two different incident geometries, $\theta_i=45°$ and 65°, were used. Figure 7 shows the neutralization of Na for four different scattering geometries: $\theta_i=55°$ and $\theta_f=55°$ (open circles), $\theta_i=55°$ and $\theta_f=75°$ (open squares), $\theta_i=75°$ and $\theta_f=55°$ (solid circles), and $\theta_i=75°$ and $\theta_f=75°$ (solid squares). In this case, the two sets of data with $\theta_f=75°$ are similar, as are the two sets of data with $\theta_f=55°$. However, note that the neutralization versus perpendicular velocity is different for the two different *final* scattering angles. From these data and the data in Figs. 4 and 6, we conclude that the neutralization does not depend on the incoming trajectory of the scattered atom. These data are consistent with the idea that the atoms lose memory of their incident charge states due to the strong interaction with the surface during the scattering. (This also indicates that the neutral detector, for which a loss of memory is assumed to occur at the Pt foil, should work as expected.)

By varying the final scattering angle, we can investigate the dependence of the final charge state on the perpendicular and parallel velocity of the outgoing atom. Figure 8(a) shows the measured neutralization probability for Na scattered from Cu(001) as a function of perpendicular velocity for several final scattering angles. The Na data with the more normal exit angles [$\theta_f=45°$ (solid triangles) and 55° (open circles)] lie essentially on the same curve, while the data for the more grazing scattering angles [$\theta_f=65°$ (×'s), $\theta_f=70°$ (open diamonds), and $\theta_f=75°$ (open squares)] do not. At the lowest velocities, all the data lie on the same curve, while at higher perpendicular velocities, the atoms with larger parallel velocities show more neutralization. The curves diverge at a perpendicular velocity of ~ 0.006 a.u. Recall that, in the BN model, since the energy and width of the atomic resonance depend only on the distance of the atom from the surface, all scattering geometries should give the same neutralization probability for a given perpendicular velocity.

Figure 8(b) shows the measured neutralization for Li scattered from Cu(100) for four different scattering geometries: $\theta_i=55°, \theta_f=55°$; $\theta_i=45°, \theta_f=45°$; $\theta_i=65°$, $\theta_f=45°$; $\theta_i=55°, \theta_f=75°$. In this case, the data from the first three geometries all lie on essentially the same curve, while the more grazing exit angle ($\theta_f=75°$) gives somewhat different results, although the differences are not as striking as they were for Na. In the following section, we

will discuss a modification to the BN model which includes a more detailed treatment of the relative motion of the atom and the metal.

V. Galilean transformations and their effect on resonant charge exchange

So far, in our model we have considered only the velocity component of the atom that is perpendicular to the surface and its role in the dynamics of the charge transfer. However, the parallel velocity of the atom can also be important [see Fig. 8(a)]. The BN model of resonant charge transfer, discussed above, was developed assuming that the metal and the scattered atom are in the same rest frame, which is not true. The motion of the atom with respect to the surface changes the charge-transfer probabilities because, from the rest frame of the atom, the energies of the metal electrons are shifted from their values in the rest frame of the metal, changing the apparent occupation of the metallic states that satisfy the resonance condition. Since the charge transfer is particularly sensitive to those electrons near the Fermi level, small changes in the apparent occupation near the Fermi level can cause significant changes in the charge-transfer probabilities.

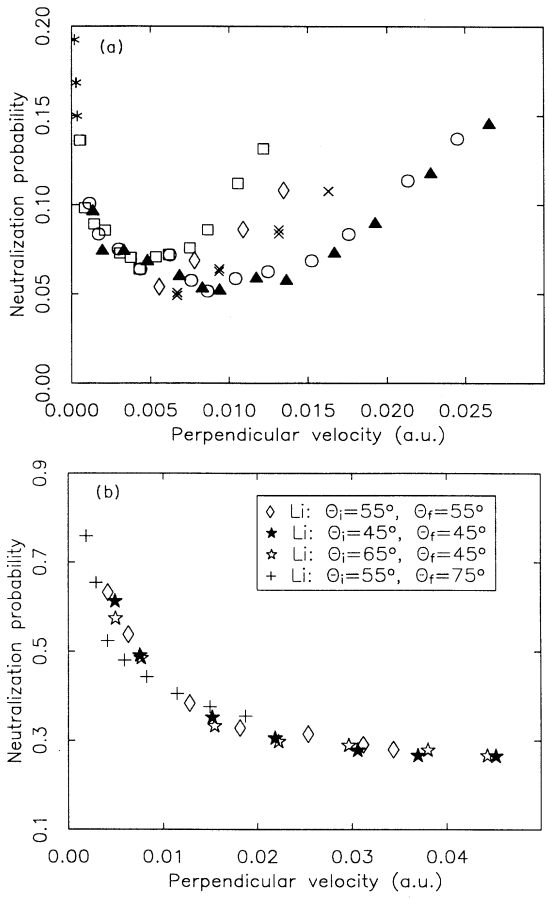

FIG. 8. Measured neutralization probability versus perpendicular velocity for Na and Li scattered from Cu(001) along the ⟨100⟩ azimuth. (a) For Na, the scattering geometries are $\theta_i=\theta_f=45°$ (solid triangles), $\theta_i=\theta_f=55°$ (open circles), $\theta_i=55°$ and $\theta_f=65°$ (×'s), $\theta_i=55°$ and $\theta_f=70°$ (open diamonds), and $\theta_i=55°$ and $\theta_f=75°$ (open squares). Data taken at low energies and very grazing scattering geometries (asterisks) show increased neutralization. Since in the BN model the resonance energy and width depend only on the distance of the atom above the surface, the neutralization depends only on the component of the velocity of the scattered atom that is perpendicular to the surface, and changing the scattering geometry should have no effect beyond changing the perpendicular velocity. Clearly, the BN model does not explain these data. (b) For Li, four different scattering geometries were used. As with the Na data (a), the data for which $\theta_f=45°$ or 55° are similar, while the data for $\theta_f=75°$ are slightly different.

In previous works where these effects are discussed, the experiments were carried out in very glancing scattering geometries.[51–53] In the experiments reported here, more normal scattering geometries are included. We are also working at lower parallel velocities than those used in previous experiments.

In what follows we will investigate how changing reference frames influences the charge-transfer calculations. We will find that the theory of resonant charge exchange based on the Newns-Anderson Hamiltonian adequately accounts for the geometry dependence of the Na neutralization seen in Figs. 7 and 8(a) provided that the Galilean transformation is included.

To understand how the velocity of the scattered atom changes the neutralization process, consider how the coupling between the atomic and metallic states, V_{ak}, changes when the Galilean transformation is included. In that case

$$V_{ak}=\langle\Psi_a|G^{\dagger}(\mathbf{v},t)V(\mathbf{x}-\mathbf{v}t)|\Psi_k\rangle \tag{8a}$$

$$=\langle\Psi_a|V(\mathbf{x})G(\mathbf{v},t)|\Psi_k\rangle\ , \tag{8b}$$

where $\mathbf{x}$ and $\mathbf{v}$ are the position and velocity of the scattered atom, $|\Psi_a\rangle$ and $|\Psi_k\rangle$ are the wave functions for the atomic and metallic states, respectively, $G(\mathbf{v},t)$ is the Galilean transformation operator, and $V(\mathbf{x})$ is the atomic potential. Equation (8a) is from the rest frame of the metal, while Eq. (8b) is from the rest frame of the atom. For free-electron-like states near the Fermi level,

$$\langle\mathbf{x}|\Psi_k\rangle\propto\begin{cases}e^{i\mathbf{k}\cdot\mathbf{x}}, & z<0\\ e^{i\mathbf{k}_{\parallel}\cdot\mathbf{x}}e^{-\delta z}, & z>0\end{cases} \tag{9a}$$

and

$$\langle\mathbf{x}|G(\mathbf{v},t)|\Psi_k\rangle\propto\begin{cases}e^{i(\mathbf{k}-\mathbf{v})\cdot\mathbf{x}}, & z<0\\ e^{i(\mathbf{k}_{\parallel}-\mathbf{q})\cdot\mathbf{x}}e^{-iv_z z}e^{-\delta z}, & z>0\ ,\end{cases} \tag{9b}$$

where $\mathbf{k}_{\parallel}$ is the component of $\mathbf{k}$ parallel to the surface, $\mathbf{q}$ is the component of $\mathbf{v}$ parallel to the surface, $z<0$ is inside the metal, and $z>0$ is outside the surface. In our experiments, $v\ll k_f$ and $v\ll\delta$. In addition, the states which are most likely to participate in the charge exchange have a wave vector $\mathbf{k}$ which is normal or nearly normal to the surface (i.e., $\mathbf{k}_{\parallel}$ is small), since those are the states which penetrate farthest into the vacuum. Therefore, $|\mathbf{k}_{\parallel}|\sim|\mathbf{q}|$ for many of the important states, and including the effect of the parallel component of the scattered atoms velocity can appreciably change the coupling

between these states and the atomic state. On the other hand, since $v \ll \delta$ for any angle of $\mathbf{k}$ with respect to the surface, $e^{iv_z z}$ is approximately one over the relevant distances and, therefore, the change in the coupling due to the velocity of the atom normal to the surface is small.

It can be shown that these changes in the coupling between the atomic and metallic states are equivalent to using the unperturbed couplings, V_{ak}, but with different energies for the metallic states. In other words, from the rest frame of the atom, the energies of the metallic states are shifted, changing the apparent occupation of the states which are resonant with the atomic state.[51,54] The energy shift can be visualized as a shift of the Fermi surface (sphere for simplicity) in k space along the direction of the scattered atom's parallel velocity.[51–53] In this picture (Fig. 9), the change in occupation of the metallic states which are resonant with the atomic level is easily seen. The atomic resonance can be represented in k space as a shell of radius $k_a = \sqrt{2\epsilon_a}$ and width Δ/k_a. The origin is taken to be the center of the resonance shell in the rest frame of the atom. For a given $\mathbf{k}$, the corresponding state in the metal is occupied if it lies within the shifted Fermi sphere and unoccupied if it does not (assuming the temperature of the metal is zero). Thus, in Fig. 9, the occupied states in the metal which are in resonance with the atomic state are given by the intersection of the resonance shell and the shaded Fermi sphere.

Van Wunnik *et al.* developed a model of resonant charge transfer, based on the Newns-Anderson Hamiltonian [Eq. (4)], which includes the parallel velocity of the atom.[51] Using the same approximations as those used in the BN model [see Sec. III B and Eq. (6)], they derived the following expression for the occupancy of the atomic orbital:

$$n_a(t) = \sum_k f_{\mathbf{k}+\mathbf{q}}(T) |V_{ak}|^2 \left| \int_{t_0}^{t} u(t') \exp\left[-i\varepsilon_k t' - \int_{t'}^{t} [i\varepsilon_a(t'') + \Delta(t'')] dt'' \right] dt' \right|^2 , \tag{10}$$

where $\mathbf{q}$ is the *parallel* velocity of the scattered atom, $|V_{ak}|^2 u(t) = \Delta(t)$, and f_{k+q} is the Fermi function which has been modified to include the shift of the Fermi sphere as described above. Equation (10) assumes that the memory of the initial state is lost.

The matrix element between the atomic state and metallic state V_{ak} depends on the angle of the metal electron's k vector with respect to the surface normal θ_k. In the BN model, this angular dependence is unimportant since the energy of the metal electron does not depend on θ_k. However, once the Galilean transformation is included, from the rest frame of the atom the energies of the metal electrons do depend on θ_k. Therefore, the angular dependence of V_{ak}, which was included implicitly in the BN model, needs to be considered explicitly.

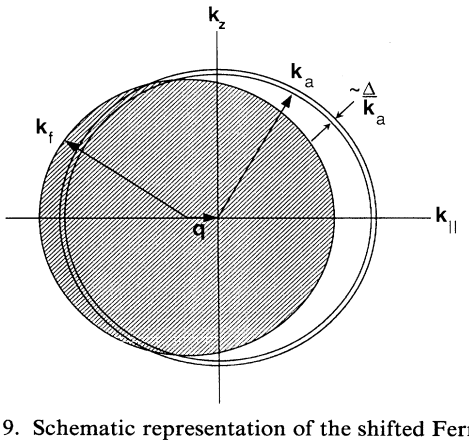

FIG. 9. Schematic representation of the shifted Fermi sphere (see the text). In k space, the atomic resonance is represented as a shell of radius $k_a = \sqrt{2\epsilon_a(z_{\rm fr})}$ and thickness Δ/k_a. The Fermi sphere of radius k_f is shifted by the parallel component $\mathbf{q}$ of the velocity vector of the scattered atom. Neutralization of the scattered atom increases when the resonance shell overlaps the shifted Fermi sphere.

Accurate calculations of the angular dependence of V_{ak} are not available. However, approximate forms have been calculated by assuming Bloch-type wave functions for the metallic states and simple hydrogenic wave functions for the atomic state.[37,52,55] We will assume that $|V_{ak}|^2$ is of the form

$$|V_{ak}|^2 = A(k) \cos^2\theta_k e^{-\alpha z} e^{-\beta k^2 \sin^2\theta_k} . \tag{11}$$

Since Eq. (10) was derived by assuming the broadband limit, $A(k)$ is chosen such that

$$\pi \sum_k |V_{ak}|^2 \delta(\epsilon - \epsilon_k) = \frac{1}{8\pi^2} \int |V_{ak}|^2 \delta(\epsilon - \epsilon_k) d^3k = \Delta(z) , \tag{12}$$

i.e., as in the BN model $\Delta(\epsilon, z) = \Delta(z)$. In Eq. (11), β is a parameter which controls the angular dependence of the matrix elements. The metallic states with small θ_k (i.e., more normal to the surface) couple more strongly to the atomic state than those with large θ_k. As β increases, the matrix elements become more sharply peaked toward the surface normal, and the states with small θ_k become relatively more important. In the Appendix, we show how we arrived at the approximate form for $|V_{ak}|^2$ [Eq. (11)]. We also show that a reasonable choice for β is $\beta = 2z_{\rm fr}/\alpha$, where $z_{\rm fr}$ is the freezing distance [Eq. (3)] and α is the inverse decay length for the coupling of the atomic and metallic states [see Eq. (2)]. However, given the approximate nature of Eq. (11), we will treat β as a parameter allowing us to test the sensitivity of the model to the angular dependence of the matrix elements. We have also considered other forms for $|V_{ak}|^2$ and found the calculated neutralization probabilities to be qualitatively similar

to those which we will present below. Thus, it is important to include the fact that the metallic states with wave vectors which are more normal to the surface couple more strongly to the atomic state, but the details of the angular dependence will not influence our conclusions.

For K, the parallel velocity model predicts less than 1% neutralization over the velocity range of our experiment, in agreement with the data. However at higher velocities, some neutralization is expected as the Fermi sphere is shifted enough to bring it into resonance with the K(4s) level. Algra *et al.* have measured the neutralization of Li, Na, and K scattered from Cu(100) in the energy range from 2 to 10 keV.[7] For their experiment, the total scattering angle was fixed at 30°, and most of the data were taken with $\theta_i=\theta_f=75°$ (angles measured with respect to the surface normal). Since the final neutralization is independent of the incident trajectory (Fig. 7), we can compare their data with ours for the cases where $\theta_f=75°$.

Figure 10 shows the K data from both experiments. At low velocities, no neutralization is seen, but at higher velocities, the data of Algra *et al.* show the onset of neutralization. The BN model predicts less than 1% neutralization for K in the velocity range shown in Fig. 10. Therefore, the increase in neutralization is not due to an increase in the level width, but rather due to the shifted Fermi sphere.

Along with the data in Fig. 10, we have shown the results of the parallel velocity model [Eq. (10)] for $\theta_f=75°$

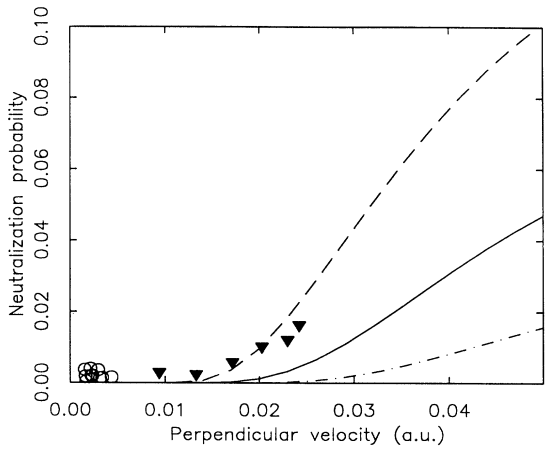

FIG. 10. Neutralization probability versus perpendicular velocity for K. Algra *et al.* (Ref. 7) have measured the neutralization probability for K scattered from Cu(001) along the ⟨100⟩ azimuth with $\theta_i=\theta_f=75°$ (solid triangles). We compare these data to our measured K neutralization probabilities for which $\theta_i=55°$ and $\theta_f=75°$ (open circles). Also shown are calculations using the model which includes the Galilean transformation [Eq. (10)]. At higher velocities, the shifted Fermi sphere causes some neutralization which is seen both in the data of Algra *et al.* and in the model. In the model, the velocity dependence of the neutralization is sensitive to the angular dependence of the coupling β. Three calculated curves are shown, one using $\beta=2z_{\rm fr}/\alpha$ (solid line), and two others using $\beta=z_{\rm fr}/\alpha$ (dashed line) and $\beta=4z_{\rm fr}/\alpha$ (dash-dotted line). Using $\beta=z_{\rm fr}/\alpha$ gives the best agreement with the data.

when the parameter β was taken to be $\beta=2z_{\rm fr}/\alpha$ as well as for values of β which are twice and half as large. The velocity at which K begins to neutralize is sensitive to the choice of β, i.e., to how sharply peaked the matrix elements are toward the surface normal. For larger β, the matrix elements are more sharply peaked, and higher parallel velocities are required to cause neutralization. The model with $\beta=z_{\rm fr}/\alpha$ (dashed line) gives a reasonable fit to the data.

Figure 11(a) shows our Li neutralization data [same as Fig. 8(b)] and the results of the parallel velocity model [Eq. (10)] with $\beta=z_{\rm fr}/\alpha$. The different scattering geometries give only slightly different results as is seen in the data. Good agreement between the theory and the data is achieved using the parallel velocity model with the energy and the lifetime given by Eqs. (1) and (2) which were fit to the calculations of Nordlander and Tully.[20,50]

Figure 11(b) shows the Na neutralization data [same as Fig. 8(a)] and the parallel velocity model [Eq. (10)] with $\beta=z_{\rm fr}/\alpha$. The energy and lifetime calculated by Nordlander and Tully[20,50] were fit to Eqs. (1) and (2), respectively. [Note that the BN model results shown here are slightly different than those in Fig. 6 where the tabulated values of $\epsilon_a(z)$ and $\Delta(z)$ were used without fitting to Eqs. (1) and (2).] Including the parallel velocity improves the agreement between the theory and the data relative to that obtained with the BN model (solid line). In particular, including the parallel velocity qualitatively reproduces the geometry dependence of the neutralization which is seen in the data. For Na, even at very low perpendicular velocities ($v_z\approx0.01$), the neutralization is sensitive to changes in the parallel velocity.

The importance of slight shifts of the Fermi sphere (i.e., corresponding to the low parallel velocities in our experiments) can be understood most easily with the aid of the freezing distance model and Fig. 9. For Na, at the lowest perpendicular and parallel velocities, the freezing distance is far from the surface, and the resonance shell is nearly concentric with, and just smaller than, the Fermi sphere (i.e., the energy of the resonance is just below ϵ_f at the freezing distance). Therefore, the neutralization probability is appreciable. At slightly higher perpendicular velocities, the freezing distance decreases so that the resonance shell is now larger than the Fermi sphere [$\epsilon_a(z_{\rm fr})>\epsilon_f$] and, since the resonance is still fairly narrow, the neutralization decreases. In the BN model, the neutralization begins to increase slowly again at higher perpendicular velocities as the freezing distance decreases further and the resonance broadens (i.e., the resonance shell in Fig. 9 gets broader). However, in the model which includes the shifting of the Fermi sphere, the neutralization increases more rapidly with increasing velocity because the shifted Fermi sphere begins to overlap with the resonance shell. For a given perpendicular velocity, the increase in the neutralization becomes more pronounced as θ_f increases, and the Fermi sphere is shifted more. Since, for the case of Na, $\epsilon_a(z_{\rm fr})\approx\epsilon_f$, very small shifts of the Fermi sphere will cause overlap.

Figure 12 shows the Li and Na data for $\theta_f=75°$ from Figs. 8(a) and 8(b) and from Algra *et al.*[7] In Fig. 8(b),

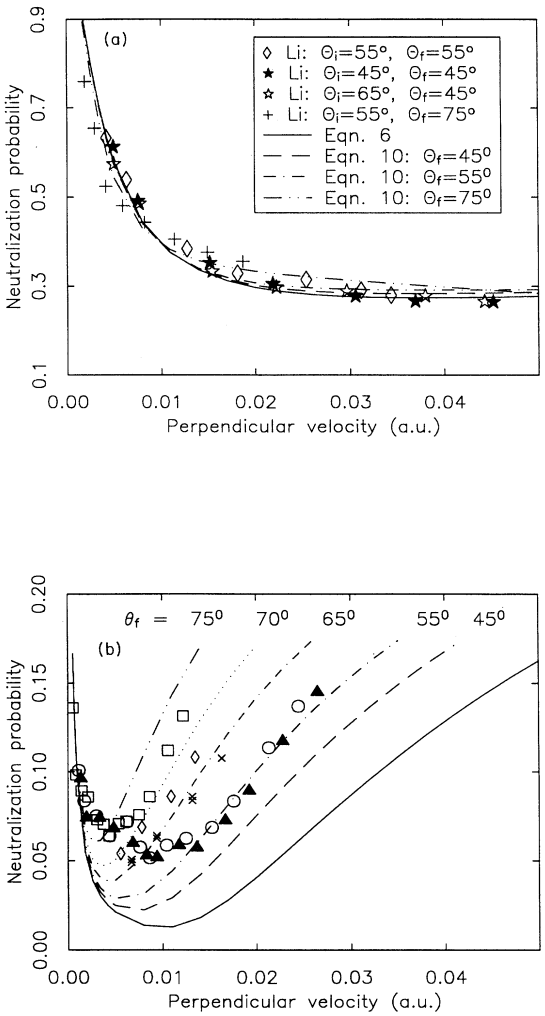

FIG. 11. Comparison of the measured Li and Na neutralization probabilities versus perpendicular velocity to calculations using a charge exchange model which includes the parallel component of the scattered particle's velocity, i.e., includes the Galilean transformation between the atom and the surface [Eq. (10)]. (a) For Li, the data were taken with four different scattering geometries [same as Fig. 8(b)]. The modeling [Eq. (10)] was done for three different final scattering angles. The results of the BN model, i.e., Eq. (6), are also shown for comparison. For Li, the effect of the Galilean transformation on the calculated neutralization probability is small. The agreement between the model, which has no free parameters, and the data is good. (b) For Na, the data were taken with five different scattering geometries: $\theta_i=\theta_f=45°$ (solid triangles), $\theta_i=\theta_f=55°$ (open circles), $\theta_i=55°$ and $\theta_f=65°$ ($\times$'s), $\theta_i=55°$ and $\theta_f=70°$ (open diamonds), and $\theta_i=55°$ and $\theta_f=75°$ (open squares). Calculated neutralization probabilities are shown for five different θ_f values, as indicated. Even at the relatively low velocities of these experiments ($v \ll v_F$, where v_F is the Fermi velocity), it is important to include the Galilean transformation in the modeling. [The results of the BN model (solid line) are also shown for comparison.] When the Galilean transformation is included, the model qualitatively reproduces the Na data. As θ_f increases, the shifted Fermi sphere increases the neutralization probability.

note that for the case of Li with $\theta_f=45°$ and 55° and perpendicular velocities of $v_z \gtrsim 0.02$ a.u., the neutralization probability changed relatively slowly with increasing perpendicular velocity. In Fig. 12 this "plateau" in the neutralization is evident in the data and is reproduced by the parallel velocity model [Eq. (10)]. For Na, this plateau in the neutralization at higher velocities (Fig. 12) is again apparent in both the data and the parallel velocity model. Our data are consistent with those of Algra *et al.* It should be noted that the higher energy Li and Na data[7] were taken with heated substrates (540 K) while our data were obtained with the sample at room temperature. Increasing the temperature increases the neutralization,[56] which could account for some of the apparent discontinuity between the two sets of data.

Given the approximations in the model and the fact that we have not attempted to adjust the level width $\Delta(z)$ to fit the data, the overall agreement (Figs. 10–12) between the parallel velocity model and the data is quite good. (Recall from Fig. 4 that the model is sensitive to the level width). In particular, the minimum in the Na neutralization as a function of velocity is reproduced at approximately the correct velocity and with the right magnitude. In addition, the plateau at higher velocities is reproduced, also with the right magnitude. Although the model depends slightly on the value of β, which was chosen using simple physical arguments (see the Appen-

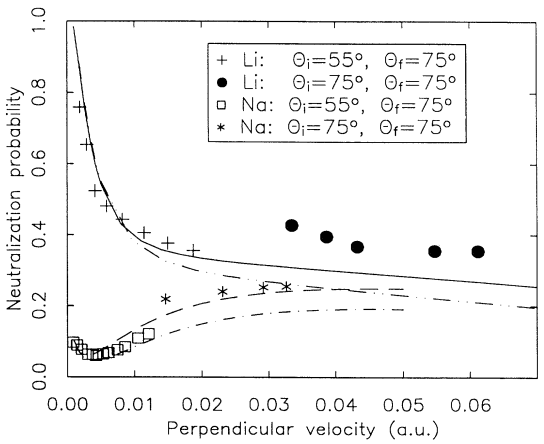

FIG. 12. Neutralization probability versus perpendicular velocity for Li and Na. Algra *et al.* have measured the neutralization probability for Li and Na scattered from Cu(001) along the ⟨100⟩ azimuth with $\theta_i=\theta_f=75°$ (Li, solid circles; Na, asterisks). Our data for Li (+'s) and Na (□) are both measured with $\theta_i=55°$ and $\theta_f=75°$. The model is shown for two choices of the coupling, $\beta=2z_{fr}/\alpha$ (Li, $-\cdots-\cdots$; Na, $-\cdot-\cdot$) and $\beta=z_{fr}/\alpha$ (Li, solid line; Na, dashed line). For this grazing scattering geometry, the parallel velocity model [Eq. (10)] reproduces the minimum in the neutralization of Na at low velocities and the plateau at higher velocities. Recall from Fig. 11(b) that the parallel velocity model also does a good job of reproducing the neutralization of Na atoms scattered in more normal scattering geometries. For Li, the model reproduces the initial rapid decrease in neutralization at the lowest velocities shown in the figure and the plateau at higher velocities.

dix), increasing or decreasing β by a factor of 2 does not qualitatively change the behavior of the model.

VI. CONCLUSIONS

We have measured the neutralization of Li, Na, and K scattered from Cu(001)⟨100⟩ as a function of velocity and scattering geometry. The neutralization as a function of perpendicular velocity P^0 is qualitatively different for each species. For Li, the neutralization monotonically decreases as the velocity increases and $0.25 \leq P^0 \leq 0.75$ for the velocities investigated. For K, essentially no neutralization is found. For Na, the neutralization versus perpendicular velocity has a minimum and $0.04 \leq P^0 \leq 0.15$ in the velocity range investigated.

We found that the BN model of resonant charge exchange based on the Newns-Anderson Hamiltonian reproduces the qualitative features of the Li, Na, and K neutralization data. In order to obtain good quantitative agreement between the theory and the data, it was necessary to include the effect of the scattered atom's parallel velocity (i.e., include the shifted Fermi sphere which results from the Galilean transformation between the rest frames of the atom and the metal). This effect was significant even at very low velocities ($v \approx 0.01 v_f$) and nonglancing scattering geometries (e.g., $\theta_f = 45°$). We found that the model of resonant charge exchange which included the shift of the Fermi sphere reproduced our data as well as that of Algra *et al.*[7]

We showed that the minimum in the neutralization probability for Na versus perpendicular velocity is due to two effects. First, as the perpendicular velocity increases, the freezing distance decreases and the width of the resonance increases. This increases the fraction of the resonance which lies below the Fermi level, thus increasing the neutralization. Second, as the parallel velocity increases, the shifted Fermi sphere increases the overlap of the occupied states in the metal with the atomic resonance, increasing the neutralization.

Most of the modeling was done with level widths $\Delta(z)$ and energies $\epsilon_a(z)$ taken from the calculations of Nordlander and Tully.[20,50] In these cases the modeling, which had no free parameters, gave excellent qualitative and good quantitative agreement with the data. We also found that it is usually reasonable to approximate the distance dependence of the level width by a simple exponential and the energy shift with a classical image shift.

In general, we have found that low and hyperthermal energy alkali-metal ion scattering from metal surfaces provides an excellent system for investigating the dynamics of the resonant charge exchange process. The knowledge gained in these experiments will be useful in understanding future experiments on more complicated systems.

ACKNOWLEDGMENTS

The authors would like to thank David Goodstein, Ernie Behringer, Peter Nordlander, and Jim Sethna for useful discussions. We also thank Ernie Behringer for a careful reading of this manuscript. G.A.K. was supported by AFOSR-91-0137 (and -88-0069) and NSF-DMR-8451979. Additional funds for the research came from NSF-DMR-9007799 and the Cornell Materials Science Center.

APPENDIX

In this appendix, we will show how we arrived at the forms for $|V_{ak}|^2$ [Eq. (11)] and β which were used in the parallel velocity model [Eq. (10)]. Approximate forms for $|V_{ak}|^2$ have been calculated by assuming Bloch-type wave functions for the metallic states and simple hydrogenic wave functions for the atomic state.[37,52,55] For that case, we have

$$|V_{ak}|^2 \propto A(k)\cos^2\theta_k e^{-2\delta z}, \tag{A1}$$

where θ_k is the angle of k with respect to the surface normal; $\delta = \sqrt{2(V_b - \epsilon_k) + k_\parallel^2}$, where $-V_b$ is the energy of the bottom of the valence band with respect to the vacuum; ϵ_k is the energy of the metal electron with respect to the bottom of the band; and $k_\parallel$ is the component of k parallel to the surface. If we define $-\epsilon$ as the energy of the electron measured from the vacuum, then $\delta = \sqrt{2\epsilon + k^2 \sin^2\theta_k}$.

In Eq. (A1), the k and z dependences are not separable as was assumed in the derivation of the BN model. However, following van Wunnik *et al.*,[51] Eq. (A1) can be approximated by

$$|V_{ak}|^2 \propto A(k)\cos^2\theta_k e^{-2\sqrt{2\epsilon}z} e^{-zk^2\sin^2\theta_k/\sqrt{2\epsilon}}. \tag{A2}$$

We can replace z in the last term of this equation with $z_{\rm fr}$ [Eq. (3)], and since the electrons at the Fermi level penetrate farthest into the vacuum, we can replace ϵ with φ, the work function of the metal.[51] Therefore,

$$|V_{ak}|^2 \propto A(k)\cos^2\theta_k e^{-2\sqrt{2\varphi}z} e^{-z_{\rm fr}k^2\sin^2\theta_k/\sqrt{2\varphi}}. \tag{A3}$$

In Eq. (A3), the k and z dependences are separable, and $A(k)$ is chosen so that the broadband approximation is fulfilled. (It is important to note that the broadband approximation for the case where the Galilean transformation is included is no more severe than in the BN model. As with the BN model, the broadband approximation is at least partially justified by the fact that the charge transfer is dominated by a small range of electronic energies which are near the Fermi level.)

To estimate the parameter β in Eq. (11), we need to consider the effect of the atomic potential on the barrier between the metallic and atomic states. The decay length of the metallic wave functions outside the metal, δ^{-1}, is determined by the energy of the metallic state compared to the barrier. In the case of a clean surface with no atom outside it, this is just the energy of the metallic state relative to the vacuum. But the perturbation due to an atom outside the surface lowers the barrier through which the electron must tunnel to reach the atom.[37,55] As a result, the energy ϵ appearing in δ should be thought of as the energy of the metallic state compared to an effective barrier and φ in Eq. (A3) should be considered an effective barrier "height," $\varphi_{\rm eff}$.[55,57] Using Eq. (A3) in Eq. (12) and comparing this to Eq. (2) we have

$$\Delta(z)=\Delta_0 e^{-\alpha z} = \frac{1}{8\pi^2} e^{-2\sqrt{2\phi_{\rm eff}}z} \times \int A(k)\cos^2\theta_k e^{-z_{\rm fr}k^2\sin^2\theta_k/\sqrt{2\phi_{\rm eff}}}\delta(\varepsilon-\varepsilon_k)d^3k \ . \quad \text{(A4)}$$

Therefore, we see that $\sqrt{2\phi_{\rm eff}}=\alpha/2$. Comparing Eqs. (A3) and (11) gives

$$\beta=\frac{z_{\rm fr}}{\sqrt{2\phi_{\rm eff}}}=\frac{2z_{\rm fr}}{\alpha} \ . \quad \text{(A5)}$$

[1]A. Blandin, A. Nourtier, and D. W. Hone, J. Phys. (Paris) **37**, 369 (1976).
[2]R. Brako and D. M. Newns, Surf. Sci. **108**, 253 (1981).
[3]H. D. Hagstrum, Phys. Rev. **96**, 336 (1954).
[4]H. D. Hagstrum, Phys. Rev. **122**, 83 (1961).
[5]M. L. Yu and N. D. Lang, Phys. Rev. Lett. **50**, 127 (1983).
[6]M. L. Yu, Phys. Rev. Lett. **40**, 574 (1978).
[7]A. J. Algra, E. v. Loenen, E. P. Th. M. Suurmeijer, and A. L. Boers, Radiat. Eff. **60**, 173 (1982).
[8]H. D. Hagstrum, P. Petrie, and E. E. Chaban, Phys. Rev. B **38**, 10 264 (1988).
[9]G. A. Kimmel, D. M. Goodstein, Z. H. Levine, and B. H. Cooper, Phys. Rev. B **43**, 9403 (1991).
[10]K. W. Sulston, A. T. Amos, and S. G. Davison, Phys. Rev. B **37**, 9121 (1988).
[11]J. Los and J. J. C. Geerlings, Phys. Rep. **190**, 133 (1990).
[12]N. D. Lang, Phys. Rev. B **27**, 2019 (1983).
[13]J. J. C. Geerlings and J. Los, Phys. Lett. **102A**, 204 (1984).
[14]J. J. C. Geerlings, L. F. Tz. Kwakman, and J. Los, Surf. Sci. **184**, 305 (1987).
[15]P. W. van Amersfoort, J. J. C. Geerlings, L. F. Tz Kwakman, E. H. A. Granneman, and J. Los, J. Appl. Phys. **58**, 2312 (1985).
[16]D. M. Newns, Comments Condens. Matter Phys. **14**, 295 (1989).
[17]R. Brako and D. M. Newns, Rep. Prog. Phys. **52**, 655 (1989).
[18]N. D. Lang and J. K. Norskov, Phys. Scr. **T6**, 15 (1983).
[19]M. Remy, J. Chem. Phys. **53**, 2487 (1970).
[20]P. Nordlander and J. C. Tully, Surf. Sci. **211/212**, 207 (1989).
[21]D. M. Newns, K. Makoshi, R. Brako, and J. N. M. van Wunnik, Phys. Scr. **T6**, 5 (1983).
[22]A. Zangwill, *Physics at Surfaces* (Cambridge University Press, Cambridge, 1988).
[23]J. W. Gadzuk, L. J. Richter, S. A. Buntin, D. S. King, and R. R. Cavanagh, Surf. Sci. **235**, 317 (1990).
[24]P. Nordlander (private communication).
[25]O. Grizzi, M. Shi, H. Bu, J. W. Rabalais, and R. A. Baragiola, Phys. Rev. B **41**, 4789 (1990).
[26]H. Brenten, H. Müller, and V. Kempter, Z. Phys. D **21**, 11 (1991).
[27]R. Hentschke, K. J. Snowden, P. Hertel, and W. Heiland, Surf. Sci. **173**, 565 (1986).
[28]K. J. Snowden, R. Hentschke, A. Narmann, and W. Heiland, Surf. Sci. **173**, 581 (1986).
[29]R. Zimny, Z. L. Miskovic, N. N. Nedeljkovic, and Lj. D. Nedeljkovic, Surf. Sci. **255**, 135 (1991).
[30]D. L. Adler and B. H. Cooper, Rev. Sci. Instrum. **59**, 137 (1988).
[31]R. L. McEachern, D. L. Adler, D. M. Goodstein, G. A. Kimmel, B. R. Litt, D. R. Peale, and B. H. Cooper, Rev. Sci. Instrum. **59**, 2560 (1988).
[32]G. A. Kimmel and B. H. Cooper, Rev. Sci. Instrum. **64**, 672 (1993).
[33]C. A. DiRubio, R. L. McEachern, J. G. McLean, and B. H. Cooper (unpublished).
[34]B. H. Cooper, C. A. DiRubio, G. A. Kimmel, and R. L. McEachern, Nucl. Instrum. Methods Phys. Res. B **64**, 49 (1992).
[35]The increase in the neutral intensity at low velocities in Fig. 2 corresponds to later arrival times, which are not shown in Fig. 1.
[36]B. Rasser, J. N. M. van Wunnik, and J. Los, Surf. Sci. **118**, 697 (1982).
[37]J. W. Gadzuk, Surf. Sci. **6**, 133 (1967).
[38]As an ion leaves the surface, it slows down due to the attractive interaction with its image charge. This effect is negligible at all but the lowest velocities in our experiments, where it can have a slight affect on the neutralization probability.
[39]In fact, the atom loses memory of its charge state even a short time (or distance) before.
[40]P. O. Gartland, Phys. Norv. **6**, 201 (1972); P. O. Gartland, S. Berge, and B. J. Slagsvold, *ibid.* **7**, 39 (1973).
[41]See, for example, R. D. Levine and R. B. Bernstein, *Molecular Reaction Dynamics and Chemical Reactivity* (Oxford University Press, New York, 1987).
[42]R. Brako and D. M. Newns, Solid State Commun. **55**, 633 (1985).
[43]D. Langreth and P. Nordlander, Phys. Rev. B **43**, 2541 (1991).
[44]H. Nakanishi, H. Kasai, and A. Okiji, Surf. Sci. **197**, 515 (1988).
[45]J. B. Marston, D. R. Andersson, E. Behringer, C. A. DiRubio, G. A. Kimmel, C. Richardson, and B. H. Cooper, Phys. Rev. B **48**, 7809 (1993).
[46]J. J. C. Geerlings, R. Rodink, J. Los, and J. P. Gauyacq, Surf. Sci. **186**, 15 (1987).
[47]H. Schall, W. Huber, H. Hoermann, W. Maus-Friedrichs, and V. Kempter, Surf. Sci. **210**, 163 (1989).
[48]H. Brenten, H. Müller, K. H. Knorr, D. Kruse, H. Schall, and V. Kempter, Surf. Sci. **243**, 309 (1991).
[49]E. R. Behringer, D. R. Andersson, D. M. Goodstein, B. Kasemo, B. H. Cooper, and J. B. Marston, Nucl. Instrum. Methods Phys. Res. B **78**, 3 (1993); D. R. Andersson, E. R. Behringer, B. H. Cooper, and J. B. Marston, J. Vac. Sci. Technol. A **11**, 2133 (1993).
[50]Nordlander calculated the energies and level widths for Li and Na above a jellium surface with $r_s=2.6$ which is appropriate for copper. These energies and level widths only differ slightly from those calculated for $r_s=2$ as in Ref. 20.
[51]J. N. M. van Wunnik, R. Brako, K. Makoshi, and D. M. Newns, Surf. Sci. **126**, 618 (1983).
[52]R. Zimny, H. Nienhaus, and H. Winter, Radiat. Eff. Def. Sol. **109**, 9 (1989).

[53]R. Zimny, Surf. Sci. **233**, 333 (1990).
[54]G. A. Kimmel, Ph.D. thesis, Cornell University (unpublished).
[55]R. Brako, Phys. Rev. B **30**, 5629 (1984).
[56]E. G. Overbosch, B. Rasser, A. D. Tenner, and J. Los, Surf. Sci. **92**, 310 (1980).

[57]In reality, the barrier between the atom and the surface has a complex three-dimensional structure, so reducing this problem to a single barrier "height" is only intended to illustrate the effect.